

# A Steady-State Kinetic Model Can Be Used to Describe the Growth of Self-Assembled Monolayers (SAMs) on Gold

Young-Seok Shon and T. Randall Lee\*

Department of Chemistry, University of Houston, Houston, Texas 77204-5641

Received: February 18, 2000; In Final Form: June 15, 2000

The kinetics of formation of self-assembled monolayers (SAMs) on gold generated by the adsorption of 2,2-dipentadecylpropane-1,3-dithiol (**d-C17**,  $[\text{CH}_3(\text{CH}_2)_{14}]_2\text{C}[\text{CH}_2\text{SH}]_2$ ), 2-pentadecylpropane-1,3-dithiol (**m-C17**,  $\text{CH}_3(\text{CH}_2)_{14}\text{CH}[\text{CH}_2\text{SH}]_2$ ), and heptadecanethiol (**n-C17**,  $\text{CH}_3(\text{CH}_2)_{16}\text{SH}$ ) from 1 mM solutions in isoctane were explored. A series of systematic coadsorption studies involving these adsorbates was also examined. Similarly, the kinetics of adsorption of the corresponding disulfides, 4,4-dipentadecyl-1,2-dithiolane (**d-C17SS**,  $[\text{CH}_3(\text{CH}_2)_{14}]_2\text{C}[\text{CH}_2\text{S}]_2$ ), 4-pentadecyl-1,2-dithiolane (**m-C17SS**,  $\text{CH}_3(\text{CH}_2)_{14}\text{CH}[\text{CH}_2\text{S}]_2$ ), and diheptadecyl disulfide (**n-C17SS**,  $[\text{CH}_3(\text{CH}_2)_{16}\text{S}]_2$ ), were explored. The kinetics were monitored by optical ellipsometry, contact angle goniometry, and polarization modulation infrared reflection absorption spectroscopy (PM-IRRAS). For the formation of densely packed SAMs, the data showed two kinetic adsorption regimes: a fast initial regime in which  $\sim 80$ – $90\%$  of the monolayer was formed, followed by a slower orientational ordering regime in which the alkyl chains became more densely packed and highly crystalline. In contrast, the formation of loosely packed SAMs exhibited a single rapid adsorption regime with little subsequent change. A comparison of the kinetic and coadsorption data generated from the various adsorption studies was interpreted using a steady-state kinetic model involving an initial steady-state physisorption, followed by a chemisorption step, leading ultimately to complete monolayer formation. The relative rates of adsorption in the slow ordering regime were perhaps additionally influenced by the rates of diffusion of the adsorbates through the partially formed monolayer films.

## Introduction

Although the properties and uses of self-assembled monolayers (SAMs) of alkanethiols and dialkyl disulfides on gold are well established,<sup>1–3</sup> the fundamental adsorption mechanisms that govern SAM formation remain poorly defined. Several research groups have employed a variety of techniques to explore the intrinsic adsorption processes.<sup>4,5</sup> The proposed nature of the steps involved, however, varies widely according to the analytical method, concentration in solution, chain length of adsorbate, type of solvent, and cleanliness of gold substrate employed in the investigations.<sup>4</sup> Although at least two studies based on UHV scanning tunneling microscopy (STM) have proposed a one-step mechanism for the adsorption process,<sup>5,6</sup> most studies favor a two-step mechanism that involves a fast initial adsorption followed by a slower orientational ordering.<sup>7,8</sup> In the latter studies, the presence of an adsorbed monolayer is usually detected within a few minutes or even seconds of immersion time;<sup>9,10</sup> the longer orientational ordering process might last several hours<sup>8</sup> or even days<sup>11</sup> for SAMs formed from dilute solutions. Most studies of the kinetics of adsorption have focused on SAMs formed from normal alkanethiols, although a few reports have explored the use of structurally distinct sulfur-based adsorbates.<sup>12–14</sup>

Although the nature of the Au–S bond and the quality of the films generated from alkanethiols and dialkyl disulfides are generally regarded as indistinguishable,<sup>9,15,16</sup> recent studies have suggested distinct properties and final coverages of SAMs

generated from these two types of adsorbates.<sup>17–19</sup> Other reports have suggested different binding properties (e.g., adsorption as a dimer) for SAMs derived from disulfides compared to those derived from thiols.<sup>20,21</sup> Previous studies of the kinetics of monolayer formation and/or exchange have found, in general, that normal alkanethiols are kinetically more labile than their corresponding dialkyl disulfides.<sup>8,9,15,22</sup> The difference in rates has been attributed to (1) greater steric hindrance afforded by the large dihedral angle ( $\text{C}–\text{S}–\text{S}–\text{C} \approx 90^\circ$ )<sup>23</sup> of the disulfides,<sup>9,22</sup> (2) preferential displacement of adsorbed solvent by the thiols,<sup>8,15</sup> and/or (3) preferential chemical interactions between the thiols and the surface of gold.<sup>15,22</sup>

A major goal of our research is to understand the relationships between the kinetics of film growth and the structure of the adsorbates. These studies might lead not only to new insight into the fundamental mechanism(s) of SAM formation but also to new strategies for enhancing film performance and stability. In previous work, we explored the use of chelating sulfur-based adsorbates for generating new types of SAMs on gold.<sup>24–32</sup> In particular, we described a new chelating strategy for the generation of SAMs from 2,2-dialkylpropane-1,3-dithiols (“spiroalkanedithiols”) and 2-monoalkylpropane-1,3-dithiols.<sup>28–32</sup> SAMs derived from these adsorbates exhibited unique structural features when compared to SAMs derived from normal alkanethiols. The SAMs generated, for example, from the spiroalkanedithiols were highly oriented and well packed, but less crystalline than those generated from normal alkanethiols;<sup>28</sup> in contrast, SAMs generated from the 2-monoalkylpropane-1,3-dithiols were the least densely packed and least crystalline of all adsorbates examined.<sup>30</sup>

\* To whom correspondence should be addressed. E-mail: trlee@uh.edu.

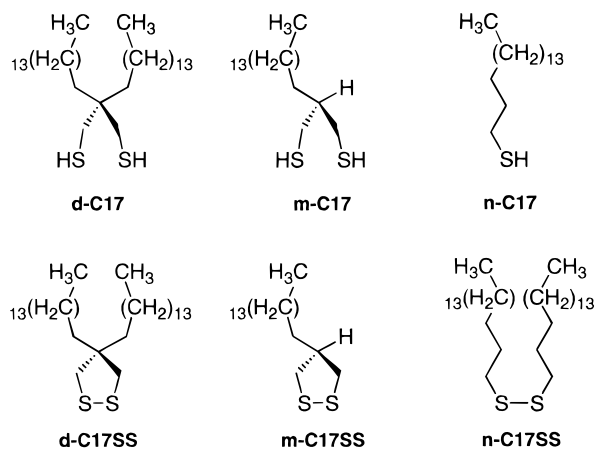


**Figure 1.** Structures of the molecules used for the adsorption studies: 2,2-dipentadecylpropane-1,3-dithiol (**d-C17**), 4,4-dipentadecyl-1,2-dithiolane (**d-C17SS**), 2-pentadecylpropane-1,3-dithiol (**m-C17**), 4-pentadecyl-1,2-dithiolane (**m-C17SS**), heptadecanethiol (**n-C17**), and heptadecyl disulfide (**n-C17SS**).

For the mechanistic studies reported here, we compare the rates of adsorption of the chelating thiols to those of normal alkanethiols having the same chain lengths (Figure 1). Our motivation for undertaking this type of comparison centered on our belief that the bulky headgroup of the spiroalkanedithiols would introduce unique steric factors that might influence both approach to and diffusion on the surface. Moreover, we felt that the low density of 2-monoalkylpropane-1,3-dithiol-based SAMs would afford enhanced permeability and thus facile approach of the adsorbate to the surface during film formation. Furthermore, we felt that the chelating nature of both adsorbates would inhibit their rates of diffusion on the surface relative to those of normal alkanethiol-based adsorbates.

In other work reported here, we compare the rates of film formation of both chelating and nonchelating thiols to those of their corresponding disulfides. We undertook these studies to examine the potential roles that steric bulk (arising from the preferred  $90^\circ$  C–S–S–C dihedral angle of normal dialkyl disulfides)<sup>23</sup> and diffusion to the surface (arising from molecular size effects during partial monolayer formation) might play during the adsorption process. To reduce or perhaps eliminate the influence of these factors, we synthesized and studied the rates of film formation for two chelating dithiols and their corresponding cyclic disulfides having C–S–S–C dihedral angles of less than  $10^\circ$  (Figure 1).<sup>33</sup> Herein, we also briefly explore the influence of solvent effects (ethanol vs isooctane) on the rates of adsorption of heptadecanethiol on gold.

## Experimental Section

The majority of the materials and experimental procedures employed here have been described in detail in previous reports.<sup>28,30</sup> The synthesis of the cyclic disulfides from the known corresponding dithiols<sup>28,30</sup> is outlined in the paragraphs below. Complete analytical data are provided for the previously unreported cyclic disulfides. In forming the SAMs, gold-coated silicon wafers were immersed in 1 mM solutions of each adsorbate dissolved in isooctane for the time intervals indicated on the kinetic plots (i.e., Figures 2–4 and 6–8). The resultant SAMs were immediately and thoroughly rinsed with toluene and ethanol and blown dry with ultrapure nitrogen before analysis. The adsorption process was monitored using data from ellipsometric thickness measurements, hexadecane contact angle measurements,<sup>34</sup> and polarization modulation infrared reflection

absorption spectroscopy (PM-IRRAS) measurements. All data were collected within 3 h after removal of the slides from solution. For a given kinetic run, the average values of ellipsometric thickness for at least six independent measurements were always within  $\pm 2 \text{ \AA}$  of those reported. Similarly, values of  $\theta_a^{\text{HD}}$  were reproducible to within  $\pm 2^\circ$  of those reported, and values of  $\nu_a^{\text{CH}_2}$  were reproducible to within  $\pm 1 \text{ cm}^{-1}$  of those reported.

**4,4-Dipentadecyl-1,2-dithiolane (d-C17SS).** A solution of 2,2-dipentadecylpropane-1,3-dithiol<sup>28</sup> (**d-C17**, 150 mg, 0.28 mmol) in 20 mL of anhydrous ethanol and 10 mL of THF was warmed to  $50^\circ\text{C}$ . To this stirred solution, iodine crystals were carefully added until a yellow-brown color was maintained. The reaction was allowed to continue for an additional 30 min at  $50^\circ\text{C}$ . The solution was then concentrated under vacuum, and the resulting oil was dissolved in 20 mL of diethyl ether. The mixture was washed with water ( $3 \times 20 \text{ mL}$ ), dried over anhydrous  $\text{MgSO}_4$ , and evaporated to dryness. The crude product was purified by column chromatography on silica gel using hexane as the eluant to give **d-C17SS** as a clear oil in 72% yield.  $^1\text{H NMR}$  (300 MHz,  $\text{CDCl}_3$ ):  $\delta$  2.88 (s, 4H,  $\text{CH}_2\text{S}$ ), 1.49–1.22 (m, 56H), 0.88 (t,  $J = 7.3 \text{ Hz}$ , 6H,  $\text{CH}_3$ ).  $^{13}\text{C NMR}$  (75 MHz,  $\text{CDCl}_3$ ):  $\delta$  31.9, 29.8–29.3 (m), 22.7, 14.1. Anal. Calcd for  $\text{C}_{33}\text{H}_{66}\text{S}_2$ : C, 75.21; H, 12.62. Found: C, 75.19; H, 12.67.

**4-Pentadecyl-1,2-dithiolane (m-C17SS).** Starting from 2-pentadecylpropane-1,3-dithiol (**m-C17**),<sup>30</sup> this cyclic disulfide was similarly obtained as a clear liquid in 67% yield.  $^1\text{H NMR}$  (300 MHz,  $\text{CDCl}_3$ ):  $\delta$  3.25 (d of d,  $J_{\text{vic}} = 7.3 \text{ Hz}$ ,  $J_{\text{gem}} = 12.0 \text{ Hz}$ , 2H,  $\text{CH}_2\text{S}$ ), 2.79 (d of d,  $J_{\text{vic}} = 8.0 \text{ Hz}$ ,  $J_{\text{gem}} = 12.0 \text{ Hz}$ , 2H,  $\text{CH}_2\text{S}$ ), 2.51 (m, 1H, CH), 1.51–1.16 (m, 28H), 0.88 (t,  $J = 7.7 \text{ Hz}$ , 3H,  $\text{CH}_3$ ).  $^{13}\text{C NMR}$  (75 MHz,  $\text{CDCl}_3$ ):  $\delta$  31.9, 29.8–29.2 (m), 22.7, 14.1. Anal. Calcd for  $\text{C}_{18}\text{H}_{36}\text{S}_2$ : C, 68.29; H, 11.46. Found: C, 68.01; H, 11.58.

## Results

**Adsorption of Thiols.** We compared the kinetics of film formation for 2,2-dipentadecylpropane-1,3-dithiol (**d-C17**) and 2-pentadecylpropane-1,3-dithiol (**m-C17**) to those of heptadecanethiol (**n-C17**); the structures of these adsorbates are shown in Figure 1. We monitored the kinetics using three techniques: ellipsometry, contact angle goniometry, and surface IR spectroscopy (PM-IRRAS). Because SAMs generated from the different adsorbates might have different structural properties and/or optical anisotropies, we chose to compare the overall adsorption profiles (i.e., the profiles from all three types of analysis) for each adsorbate rather than comparing individual data at a single immersion time.

For the adsorption of **d-C17** and **n-C17**, the ellipsometric thickness and hexadecane contact angle measurements suggest that  $\sim 80$ – $90\%$  of the monolayers formed in less than a few minutes or even seconds (Figure 2). Complete monolayer formation for **d-C17** was, however, noticeably slower than that for **n-C17**: while limiting thickness and contact angle values for the **n-C17** SAM were reached within 1 h (data not shown), limiting values for the **d-C17** SAM were reached only after 24–48 h. The PM-IRRAS data in Figure 3, which illustrate the increase in crystallinity (decrease in frequency of the  $\nu_a^{\text{CH}_2}$  band)<sup>35</sup> of the alkyl chains with immersion time, provide further support for these observations: whereas the limiting crystallinity for the **n-C17** SAM (corresponding to  $\nu_a^{\text{CH}_2} = 2919 \text{ cm}^{-1}$ ) was reached within 1 h, the limiting value for the **d-C17** SAM (ca.  $2921 \text{ cm}^{-1}$ ) was reached only after  $\sim 48 \text{ h}$ .

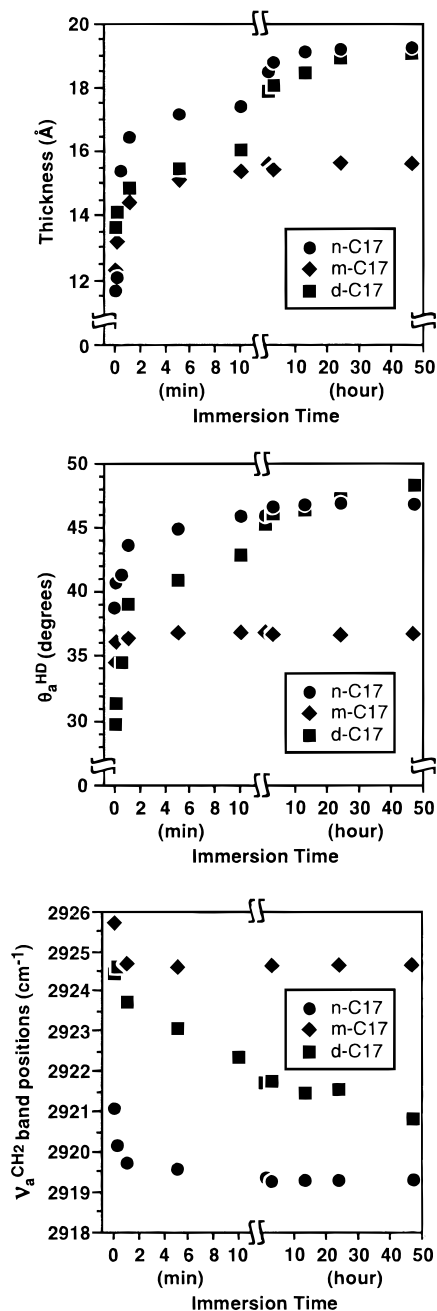


**Figure 2.** Comparison of the kinetics of monolayer formation on gold for the adsorption of 2,2-dipentadecylpropane-1,3-dithiol (**d-C17**, ■), 2-pentadecylpropane-1,3-dithiol (**m-C17**, ◆), and heptadecanethiol (**n-C17**, ●) from 1 mM solutions in isoctane.

Unlike the kinetics of film formation for **d-C17**, the adsorption of **m-C17** reached limiting coverages and crystallinities rapidly (ca. 5 min), as indicated by the ellipsometric thicknesses (ca. 15 Å), the contact angles of hexadecane (ca. 35°), and the PM-IRRAS data ( $\nu_a^{\text{CH}_2} = 2924 \text{ cm}^{-1}$ ) shown in Figure 2. Because of the low density of alkyl chains in the **m-C17** SAMs,<sup>30</sup> the limiting values are substantially different from those of **n-C17** and **d-C17** SAMs. Moreover, from these data, we cannot distinguish the relative rates of adsorption of **m-C17** vs **n-C17**; both, however, appear to adsorb markedly faster than **d-C17**.

In efforts to further discriminate the adsorption behavior of **d-C17**, **m-C17**, and **n-C17**, we explored the kinetics of adsorption under more dilute conditions (ca. 1  $\mu\text{M}$  in isoctane). Rather than providing kinetic discrimination, however, these data exhibited features that might be consistent with the

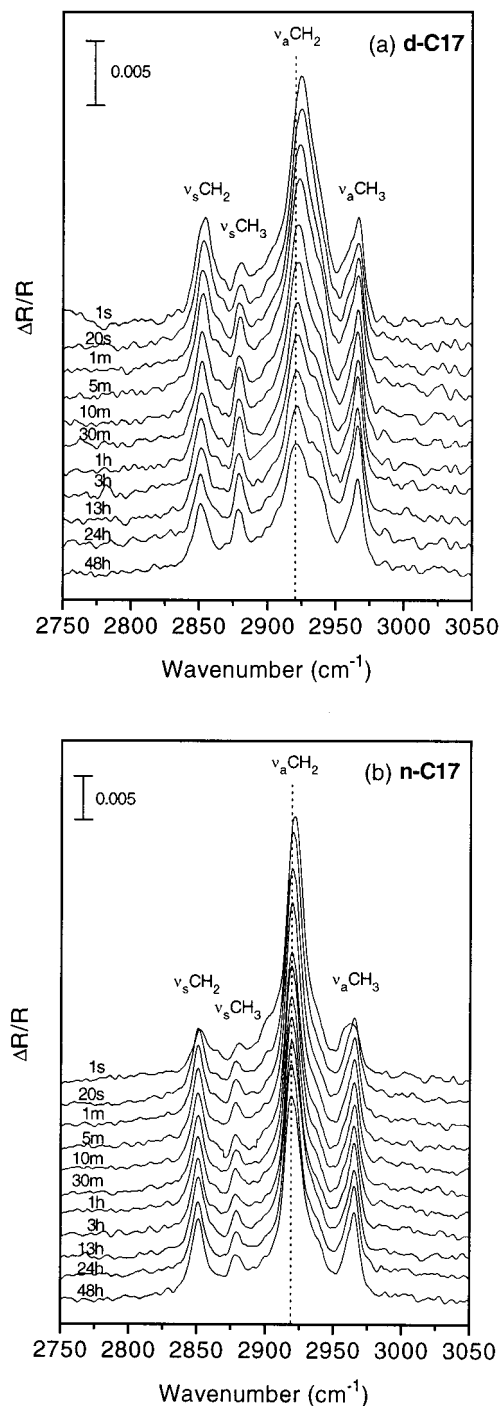


**Figure 3.** Surface infrared spectra (PM-IRRAS) of the SAMs adsorbed onto gold from 1 mM solutions of (a) **d-C17** and (b) **n-C17** in isoctane as a function of immersion time. Differential surface reflectivity ( $\Delta R/R$ ) was calculated as the ratio  $(R_p - R_s)/(R_p + R_s)$ , where  $R_p$  and  $R_s$  represent the reflectivity for the respective polarizations of light.

proposed transition from a “striped” phase to a chemisorbed state for the growth of SAMs on gold.<sup>36</sup> Examination by PM-IRRAS showed, for example, that the  $\nu_a^{\text{CH}_2}$  band appeared at  $2923 \text{ cm}^{-1}$  within a few seconds of immersion into micromolar solutions of **n-C17**; the band then slowly shifted to  $>2926 \text{ cm}^{-1}$  over the next 30 min. Surprisingly, continued immersion of the gold slides in micromolar solutions of **n-C17** failed to induce any further change in the position of the  $\nu_a^{\text{CH}_2}$  band even after several days. These data are consistent with the existence of an intermediate phase that is both disordered and stable.<sup>37</sup> The adsorption of **m-C17** under micromolar conditions showed

**TABLE 1: Data for SAMs on Gold Derived by the Adsorption and Coadsorption of C17-Thiols from 1 mM Solutions in Isooctane for 24 h<sup>a</sup>**

compound	ratio	thickness (Å)	$\theta_a^{\text{HD}}$ (°)	$\nu_a^{\text{CH}_2}$ (cm <sup>-1</sup> )
<b>d-C17</b>	—	19	47	2921
<b>d-C17/m-C17</b>	0.33	15	34	2925
	1.00	15	34	2925
	3.00	16	36	2925
<b>m-C17</b>	—	15	35	2925
<b>n-C17/m-C17</b>	0.33	15	36	2925
	1.00	16	36	2925
	3.00	15	36	2925
<b>n-C17</b>	—	19	47	2919

<sup>a</sup> Average values of ellipsometric thickness for at least six independent measurements were always within  $\pm 2$  Å of those reported. Values of  $\theta_a^{\text{HD}}$  were reproducible to within  $\pm 2^\circ$  of those reported. Values of  $\nu_a^{\text{CH}_2}$  were reproducible to within  $\pm 1$  cm<sup>-1</sup> of those reported.

similar behavior, although the exact position of the  $\nu_a^{\text{CH}_2}$  band and the time intervals involved were somewhat different than those for **n-C17** (e.g., the  $\nu_a^{\text{CH}_2}$  band shifted from 2924 to 2926 cm<sup>-1</sup> over the first 5 min of immersion). The adsorption of **d-C17** under micromolar conditions, however, showed behavior different from that of the other adsorbates: the  $\nu_a^{\text{CH}_2}$  band shifted slowly from 2927 to 2925 cm<sup>-1</sup> over the first 30 min of immersion. Prolonged immersion in the micromolar solutions, however, failed to induce complete monolayer formation for this adsorbate as was observed for the others.

**Coadsorption of Mixtures of Thiols.** For solutions containing two different thiols, preferential adsorption can plausibly be dictated by either kinetic or thermodynamic factors. Previous studies of the coadsorption of normal alkanethiols having different chain lengths demonstrated a preference for the adsorption of the thiol with the longer alkyl chain.<sup>38</sup> These results were interpreted to reflect a thermodynamic preference (arising predominantly from enhanced interchain van der Waals stabilization) for longer alkyl chain lengths. Because of the unique structural relationships between **d-C17**, **m-C17**, and **n-C17**, we felt that coadsorption studies using these adsorbates might reveal new insight into the relative influence and perhaps the origin of kinetic and/or thermodynamic discrimination in the adsorption of SAMs on gold. We reasoned, for example, that, if the adsorption were governed thermodynamically by interchain van der Waals stabilization, then the adsorption of both **d-C17** and **n-C17** would be favored over that of **m-C17**, which generates loosely packed (and thus weakly van der Waals-stabilized) films.<sup>30</sup> Furthermore, if the adsorption were governed thermodynamically by the chelate effect,<sup>39</sup> then the adsorption of both **d-C17** and **m-C17** would be favored over that of **n-C17**. Conversely, kinetic effects would favor the adsorption of both **m-C17** and **n-C17** over that of the larger, sterically bulkier **d-C17**.

First, we examined the coadsorption of **d-C17** and **m-C17** after immersion in isooctane for 1 day at room temperature (see Table 1). At ratios of **d-C17/m-C17** ranging from 1:3 to 3:1, the thicknesses, contact angles, and IR spectra were indistinguishable from those of SAMs generated solely from **m-C17**, which strongly suggests the preferential adsorption of **m-C17** over **d-C17**. Second, we examined the coadsorption of **m-C17** and **n-C17** under the same conditions. Because of their similar molecular sizes (see Figure 1) and indistinguishable rates of film formation (see Figure 2), we anticipated that any preferences observed in the coadsorption of these two thiols would be governed predominantly by thermodynamic rather than kinetic factors. The data in Table 1 strongly suggest that the

**TABLE 2: Data for SAMs on Gold Derived by the Adsorption and Coadsorption of C17-Thiols from 1 mM Solutions in Isooctane at 50 °C<sup>a</sup>**

compound	ratio	time (h)	thickness (Å)	$\theta_a^{\text{HD}}$ (°)	$\nu_a^{\text{CH}_2}$ (cm <sup>-1</sup> )
<b>d-C17</b>	—	24	19	47	2921
<b>d-C17/m-C17</b>	1.00	24	14	35	2925
		48	15	35	2925
		72	15	35	2925
	10.0	24	16	39	2924
		48	16	39	2923
		72	16	39	2923
	100	24	16	40	2923
		48	17	40	2923
		72	17	40	2923
<b>m-C17</b>	—	24	15	35	2925
<b>n-C17/m-C17</b>	1.00	24	14	35	2925
		48	15	34	2924
		72	15	34	2924
	10.0	24	14	36	2925
		48	14	35	2925
		72	14	35	2924
	100	24	14	35	2924
		48	14	35	2925
		72	14	35	2924
<b>n-C17</b>	—	24	19	47	2919

<sup>a</sup> Average values of ellipsometric thickness for at least six independent measurements were always within  $\pm 2$  Å of those reported. Values of  $\theta_a^{\text{HD}}$  were reproducible to within  $\pm 2^\circ$  of those reported. Values of  $\nu_a^{\text{CH}_2}$  were reproducible to within  $\pm 1$  cm<sup>-1</sup> of those reported.

adsorption of **m-C17** was favored over that of **n-C17** at ratios of **n-C17/m-C17** ranging from 1:3 to 3:1.

Third, we repeated the coadsorption studies at elevated temperature (50 °C), and monitored the films over the course of 3 days of immersion at 50 °C in the respective solutions (see Table 2). In studies of the coadsorption of **d-C17** and **m-C17** at ratios of **d-C17/m-C17** ranging from 1:1 to 100:1, the data suggest the preferential adsorption of **m-C17** with the relative incorporation of **d-C17** increasing with an increase in the ratio of **d-C17/m-C17**. In studies of the coadsorption of **n-C17** and **m-C17** at ratios of **n-C17/m-C17** ranging from 1:1 to 100:1, the data suggest the exclusive incorporation of **m-C17**. The invariability of these data with time is consistent with a thermodynamically controlled adsorption process, in which the relative thermodynamic stabilities are **m-C17** > **d-C17** >> **n-C17**.

**Adsorption of Thiols vs Disulfides.** To further probe the nature of the adsorption of SAMs on gold, we compared the rates of adsorption of all three thiol species to those of their corresponding disulfides. In a manner consistent with literature studies,<sup>9</sup> the ellipsometric thickness, hexadecane contact angle, and PM-IRRAS adsorption profiles showed that **n-C17SS** adsorbed at similar or perhaps marginally slower rates than **n-C17** (Figure 4). Although the final limiting thicknesses and hexadecane contact angles of the thiol-derived and the disulfide-derived SAMs were indistinguishable, the PM-IRRAS spectra show that SAMs generated from **n-C17** and **n-C17SS** have slightly different structures, as judged by the broader  $\nu_a^{\text{CH}_2}$  band for the SAM derived from the disulfide (Figure 5). This comparison suggests that the alkyl chains of SAMs derived from *n*-alkyl disulfides possess more gauche defects than those derived from *n*-alkanethiols.<sup>8,9</sup>

As for the *n*-alkyl species, the rate of adsorption of **m-C17SS** was indistinguishable from that of its thiol analogue, **m-C17** (Figure 6). Moreover, the characteristics of the final SAMs derived from both species were indistinguishable. From steric considerations, the lack of any difference between these

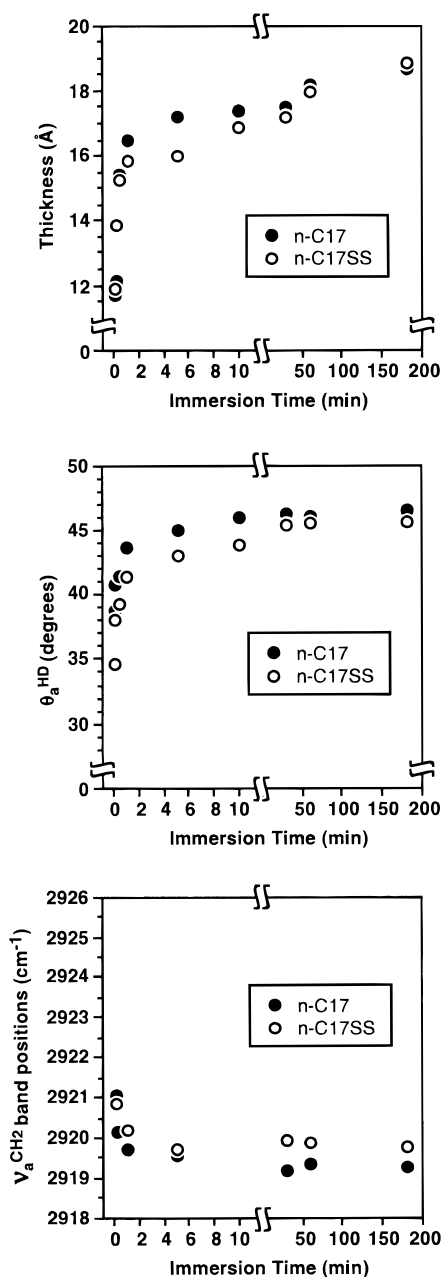


**Figure 4.** Comparison of the kinetics of monolayer formation on gold for the adsorption of heptadecanethiol (**n-C17**, ●) and heptadecyl disulfide (**n-C17SS**, ○) from 1 mM solutions in isooctane.

adsorbates is unsurprising given that the dihedral angle of **m-C17SS** is only  $\sim 2^\circ$ .<sup>33</sup> Consequently, this disulfide should present little, if any, additional steric hindrance upon approach to the surface of a partially formed film. These results are consistent with a model in which the adsorption of structurally analogous thiols and disulfides onto gold to form monolayer films will, in the absence of extraneous factors, be expected to be similar as long as the dihedral angle (and thus the steric bulk) of the disulfide is small.

In contrast to the thiol vs disulfide comparisons described above, the comparison of the adsorption profiles of **d-C17** and **d-C17SS** revealed substantial differences (Figure 7). In particular, the hexadecane contact angles and the PM-IRRAS spectra show that the adsorption of **d-C17SS** was slower than that of **d-C17**. Moreover, the limiting thickness, wettability, and crystallinity of the SAMs generated from the disulfide were less than those of the SAMs generated from the thiol. Because

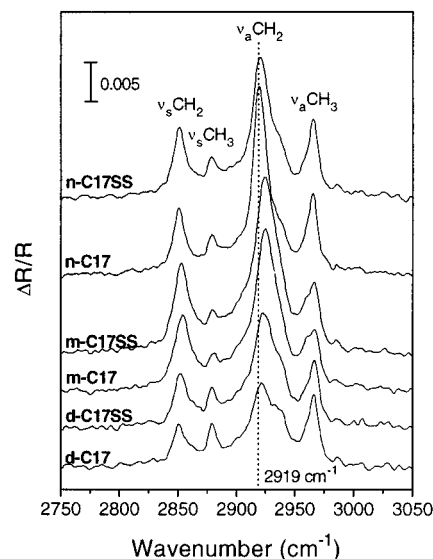


**Figure 5.** Surface infrared spectra (PM-IRRAS) of the SAMs on gold generated from the thiols and the disulfides shown in Figure 1. Differential surface reflectivity ( $\Delta R/R$ ) was calculated as the ratio  $(R_p - R_s)/(R_p + R_s)$ , where  $R_p$  and  $R_s$  represent the reflectivity for the respective polarizations of light.

**d-C17SS** possesses a small dihedral angle (ca.  $8^\circ$ ),<sup>31</sup> steric arguments appear insufficient to rationalize the observed differences.

**Solvent Effects upon Adsorption.** With only a few exceptions,<sup>40–42</sup> studies of the kinetics of SAM growth by adsorption from solution have been conducted in ethanol.<sup>4,7–11</sup> Furthermore, the kinetics of adsorption from isooctane have, to our knowledge, been unexplored even though isooctane has long been recognized as a useful solvent for the preparation of SAMs.<sup>38</sup> We used isooctane as the solvent for our initial studies of spiroalkanedithiol-based SAMs<sup>28–32</sup> because we found that these adsorbates were substantially more soluble in isooctane than in ethanol.<sup>43</sup> Moreover, to circumvent substantial solubility-related issues in the work reported here, we compared only the adsorption profiles of **n-C17** in isooctane vs ethanol in a brief exploration of the influence of solvent on the kinetics of adsorption of SAMs on gold. These data are shown in Figure 8. The thickness, wettability, and PM-IRRAS profiles demonstrate that the **n-C17** SAM reached  $\sim 90\%$  of its limiting values within a few minutes of adsorption from either ethanol or isooctane. A marginal difference in the adsorption rates was, however, detected: the adsorption of **n-C17** onto gold appeared slightly faster in ethanol than in isooctane. Correspondingly, after 3 h of immersion, the limiting thicknesses, wettabilities, and crystallinities of the SAMs showed slightly enhanced values in ethanol. Although the observed differences fell within our usual estimates of the experimental error,<sup>24–32</sup> the trends in the data were reproducible.<sup>44</sup> While it seems plausible that ethanol might dissolve strongly adsorbed polar impurities away from the surface of gold and thereby facilitate binding of the adsorbates, we cannot rule out effects arising from the coordinative association of ethanol with the surface of gold.<sup>45</sup>

## Discussion

The data presented in Figures 2 and 3 are consistent with the two-step process for the growth of SAMs on gold described in the Introduction, wherein a fast initial adsorption (the fast regime) is followed by a slower ordering process (the slow regime).<sup>7–9</sup> Recently, several reports have provided evidence that the adsorption of organosulfur compounds onto gold

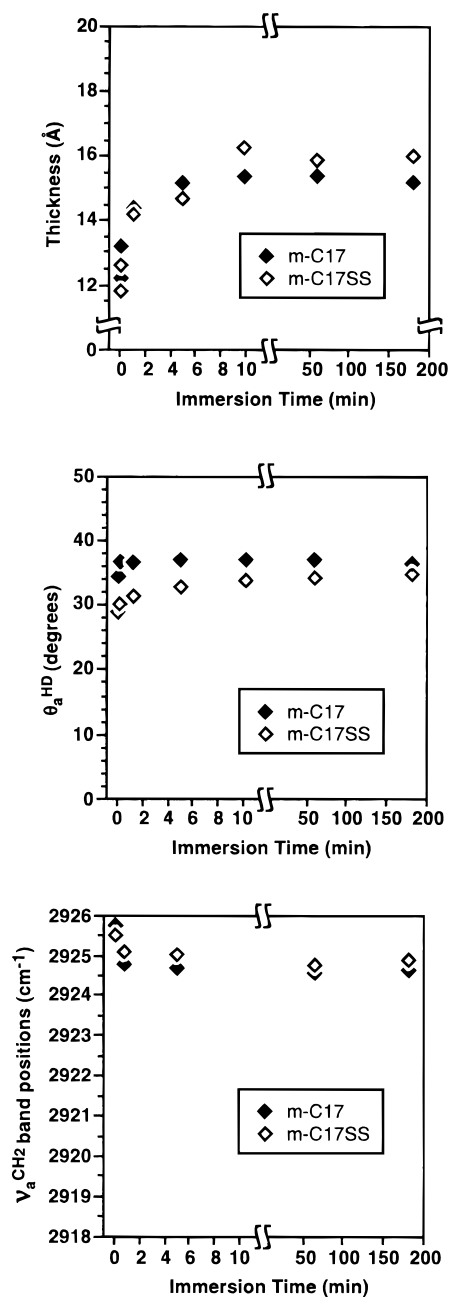
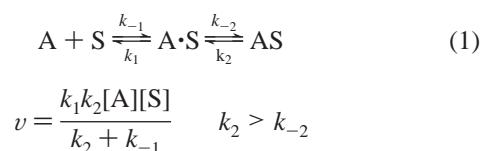


**Figure 6.** Comparison of the kinetics of monolayer formation on gold for the adsorption of 2-pentadecylpropane-1,3-dithiol (**m-C17**,  $\blacklozenge$ ) and 4-pentadecyl-1,2-dithiolane (**m-C17SS**,  $\diamond$ ) from 1 mM solutions in isoctane.

proceeds via an initial physisorbed, lying-down phase, followed by a transition to the chemisorbed state.<sup>36,37,46–49</sup> These studies were conducted using either ultrahigh vacuum vapor-phase deposition techniques<sup>36,37,46</sup> or solution self-assembly techniques.<sup>47–49</sup> We propose that the kinetic and coadsorption studies presented here (and perhaps in other related work) can be rationalized by using a steady-state approximation (eq 1). In eq 1,



A represents the adsorbate, S the surface, A·S the physisorbed

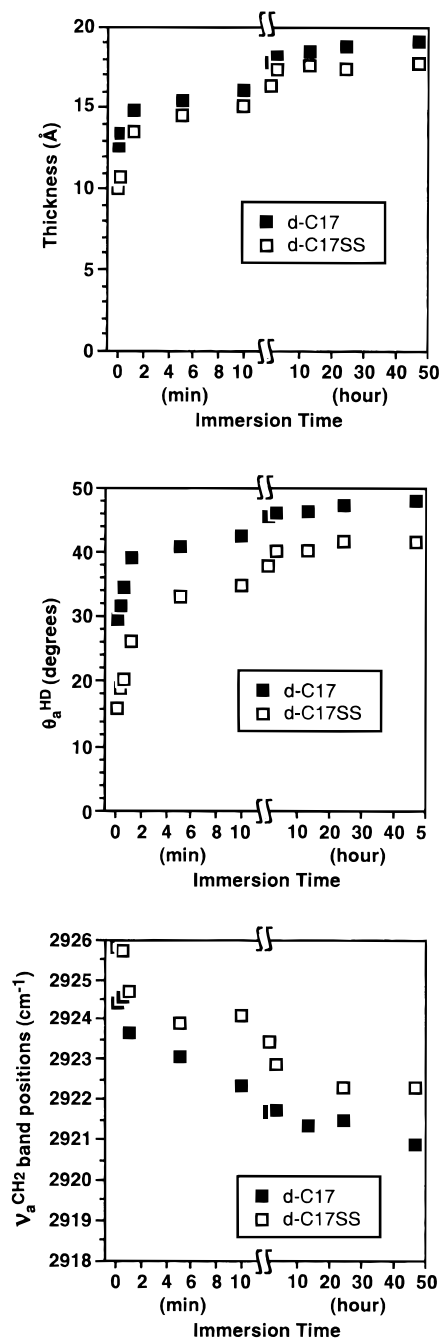


**Figure 7.** Comparison of the kinetics of monolayer formation on gold for the adsorption of 2,2-dipentadecylpropane-1,3-dithiol (**d-C17**,  $\blacksquare$ ) and 4,4-dipentadecyl-1,2-dithiolane (**d-C17SS**,  $\square$ ) from 1 mM solutions in isoctane.

intermediate, and AS the chemisorbed state.<sup>50</sup> In the gas phase or in solution at 1 mM concentrations of thiol, the rates of monolayer desorption are substantially slower than the rates of monolayer formation.<sup>7,46</sup> We can thus assume that  $k_{-2}$  is negligibly small in the present discussion. A proposed reaction coordinate diagram for the adsorption process is illustrated in Figure 9.<sup>50</sup> We can evaluate the relative rates of adsorption by examining the physisorption preequilibrium and the subsequent barrier to chemisorption. This model assumes that the relative population of the physisorbed intermediate is influenced largely by the number of methylene units composing the adsorbates and that the barrier to chemisorption is influenced by steric constraints, conformational constraints, and/or chemical factors.<sup>46,47</sup>

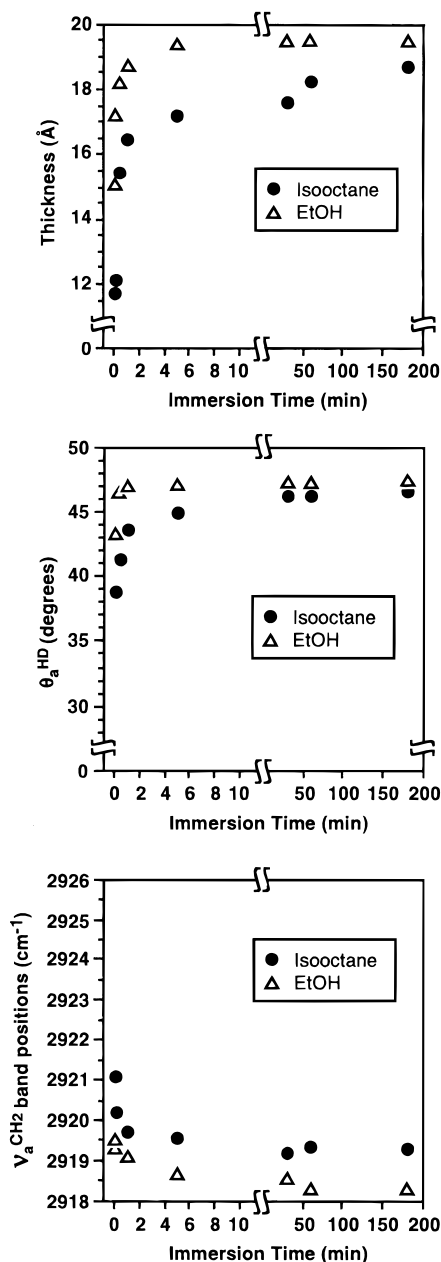


**Figure 8.** Comparison of the kinetics of monolayer formation on gold for the adsorption of 1 mM solutions of heptadecanethiol (**n-C17**) in ethanol ( $\Delta$ ) and in isooctane ( $\bullet$ ).

**Adsorption of Thiols.** In the early stages of adsorption (i.e., the fast regime), the data from the independent adsorption studies (Figure 2) suggest the following trend in the rates of adsorption of the thiols: **m-C17**  $\sim$  **n-C17** > **d-C17**. Although the kinetic data fail to distinguish differences in the rates of adsorption of **m-C17** vs **n-C17**, both of these species clearly adsorb faster than **d-C17**. Because **d-C17** contains roughly twice as many methylene groups as either **n-C17** or **m-C17**, one might expect a more highly populated physisorbed state for **d-C17** relative to those for the other two thiols,<sup>46</sup> which should correspond to a faster rate of chemisorption (i.e.,  $k_2$  in eq 1) for **d-C17** in the absence of other factors. Moreover, the two thiol groups in **d-C17** vs the one thiol group in **n-C17** should perhaps give rise to an enhanced rate of chemisorption for **d-C17** relative to that for **n-C17**. Neither of these predictions, however, is consistent with the data. Given the arguments against diffusion limitation in the early stages of SAM adsorption from solution<sup>9</sup> and the “spiro” structure of **d-C17**, we propose that its relatively

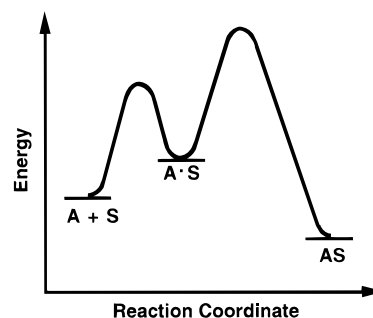


**Figure 9.** Energy diagram illustrating the two-step process for the adsorption of SAMs on gold.

slow rate of adsorption arises from steric and/or conformational constraints that limit facile chemisorption to the surface (vide infra).

In the latter stages of the adsorption process (i.e., the slow regime), at least two additional factors might also contribute to a slower rate of adsorption/orientational ordering for **d-C17** relative to that for **n-C17** and **m-C17**: (1) the rate of diffusion to the surface through the partially formed monolayer is slowest for **d-C17**, and/or (2) the rate of diffusion on the surface is slowest for **d-C17**. In the former case, the rate of diffusion of **d-C17** to the surface through the partially formed film might be restricted by the relatively large size of the adsorbate (roughly twice the size of **n-C17** or **m-C17**). In the latter case, the rate of diffusion of **d-C17** on the surface might be restricted by the chelate effect, which requires the roughly simultaneous movement of two sulfur headgroups to be overcome and is thus disfavored entropically. A third factor that must be considered is the mismatch between the maximum distance spanned by the sulfur atoms of the chelating dithiol (ca. 4.8 Å)<sup>33</sup> and the distance between the 3-fold hollow sites of Au(111) (4.99 Å), where the sulfur atoms in normal SAMs on gold are purported to bind.<sup>1,3</sup> It is possible that the underlying surface of gold must undergo a reconstruction upon the adsorption of **d-C17**, thereby slowing the rate of orientational ordering for this adsorbate.

Upon consideration of the adsorption profiles of all three thiol adsorbates, however, the data are inconsistent with either rate-limiting diffusion on the surface or rate-limiting Au reconstruction for the growth of **d-C17** SAMs on gold. If these processes were rate-limiting, then we would expect that the rates of SAM formation for **m-C17** and **d-C17** to be similar; they are not. The relative rates of adsorption in the slow ordering regime are, however, consistent with the expected relative rates of diffusion of the adsorbates to the surface through the partially formed films. In this diffusional model, the rates of adsorption in the slow ordering regime would be influenced by molecular-size-based steric factors that dictate the approach of the adsorbate to the surface. Indeed, the sizes of **n-C17** and **m-C17** are similar, and their rates of film formation are similar; the **d-C17** adsorbate is approximately twice as large as the other two, and its rate of film formation is substantially slower than those for the other two. We admit that the validity of this model rests, to some degree, on the validity of our assumption that the limiting values of the adsorption profiles in Figure 2 for the growth of the **m-C17** SAM represent “complete” monolayer formation.<sup>30</sup> The low contact angles of hexadecane and the poor crystallinities indicated by the IR data weaken this assumption.

One might argue that an enhanced permeability for the **m-C17** adsorbate (arising from its low density of alkyl chains)<sup>30</sup> could at least partially give rise to its rapid rate of film formation. Because, however, the kinetic profiles in Figure 2 suggest that

the rate of film formation for the **n-C17** SAM (whose density of alkyl chains is approximately twice that of the **m-C17** SAM)<sup>30</sup> is indistinguishable from that for the **m-C17** SAM, the data in Figure 2 provide no evidence to support this hypothesis. Moreover, the coadsorption studies, which suggest the preferential adsorption of **m-C17** over **n-C17**, shed little, if any, light on the matter (vide infra).

**Coadsorption of Mixtures of Thiols.**<sup>51</sup> The results from the coadsorption studies demonstrate that **m-C17** adsorbs preferentially over both **d-C17** and **n-C17**; in each case, the origin of the preference is either kinetic or thermodynamic in nature. Indeed, the independent adsorption studies in Figure 2 suggest a faster rate of adsorption of **m-C17** vs that of **d-C17**. Because of the anticipated stronger physisorption of **d-C17** relative to that of **m-C17** (vide supra), we would argue that any kinetic preference for **m-C17** must originate in the chemisorption step. As discussed in detail below, the steric and conformational constraints of the spiro structure of **d-C17** could perhaps rationalize its relatively slow rate of chemisorption.

Although a rationalization for the preferential adsorption of **m-C17** over **d-C17** based on kinetic factors seems plausible, a rationalization based on thermodynamic factors is more obscure. Consider, for example, the relative packing densities of the alkyl chains of complete **m-C17** and **d-C17** SAMs. The corresponding relative interchain van der Waals forces should thermodynamically favor the adsorption of **d-C17** over that of **m-C17**. Despite this argument, however, the data in Table 2 (and independent studies of SAM exchange with free thiols in solution)<sup>52</sup> suggest that the **m-C17** SAMs are thermodynamically more stable than the **d-C17** SAMs. We speculate that the thermodynamic preference for **m-C17** over **d-C17** might arise from an enhanced conformational accessibility that allows **m-C17** to bind (chelate) particularly strongly to the surface of gold.<sup>53</sup>

From a kinetics perspective, the preference for **m-C17** over **n-C17** might plausibly arise from a faster rate of chemisorption (i.e.,  $k_2$  in eq 1) for **m-C17** relative to that for **n-C17**. Because **n-C17** and **m-C17** have similar molecular structures, we infer that, unless the two sulfur moieties in **m-C17** vs the single sulfur in **n-C17** introduces a substantial perturbation,<sup>46</sup> the magnitude of physisorption should be similar for the two adsorbates. Consequently, the preferential adsorption of **m-C17** over **n-C17** might arise kinetically from their relative rates of chemisorption because of their relative stoichiometries; that is, because **m-C17** possesses two nucleophiles (two thiol groups) rather than one, **m-C17** might undergo chemisorption more readily than **n-C17**.

The preferential adsorption of **m-C17** over **n-C17** might also arise from thermodynamic factors, given that the data in Table 2 and elsewhere<sup>52</sup> suggest that the **m-C17** SAM is thermodynamically more stable than the **n-C17** SAM. However, because the SAM derived from **m-C17** is less densely packed than that derived from **n-C17**,<sup>30</sup> any thermodynamic preference for the adsorption of **m-C17** over **n-C17** must arise from factors other than interchain van der Waals stabilization. It is possible, for example, that a thermodynamic preference for **m-C17** arises from the entropy-driven chelate effect, which is known to stabilize ligand-to-metal binding in organometallic complexes.<sup>39</sup> Similarly, the preference for the adsorption of **m-C17** over **n-C17** might arise from entropic considerations if the sulfur headgroups are required to bind as dimers (i.e., disulfides) on the surface of gold in order to maximize the binding interaction.<sup>54</sup> It is further possible that **m-C17** is less soluble in isooctane than is **n-C17**, which would also favor the adsorption of **m-C17**.<sup>38</sup>

**Comparison of Thiols and Disulfides.** As noted above, previously reported faster rates of adsorption and/or replacement of thiols compared to those of structurally analogous disulfides have been attributed to the following origins:<sup>8,9,15,22</sup> (1) greater steric hindrance afforded by the large dihedral angle ( $C-S-S-C \approx 90^\circ$ )<sup>9,22</sup> of the disulfides, (2) preferential displacement of adsorbed solvent by the thiols,<sup>8,15</sup> and/or (3) preferential chemical interactions between the thiols and the surface of gold.<sup>15,22</sup> In comparisons of normal alkanethiols and disulfides, the disulfide undoubtedly possesses greater steric bulk.<sup>9</sup> Moreover, the disulfide requires the simultaneous creation of two chemisorption sites compared to one site for the thiol. However, for the chelating alkanedithiols and disulfides examined here (Figure 1), the steric bulk and surface site requirements are largely indistinguishable. Moreover, because the analogous chelating alkanedithiols and disulfides are structurally similar, the degree of physisorption is probably similar for both types of adsorbates. Consequently, we are left to conclude that chemisorption must constitute the distinguishing step in the observed faster rate of adsorption of **d-C17** relative to that of **d-C17SS** (see Figure 7).

A faster rate of chemisorption for **d-C17** relative to that for **d-C17SS** can plausibly arise from at least three factors: (1) a faster rate of oxidative addition of the two  $S-H$  bonds in **d-C17** vs the single  $S-S$  bond in **d-C17SS** to the surface of gold, (2) a retarded adsorption of **d-C17SS** due to contamination of the sample with oligomeric or polymeric disulfide species,<sup>55</sup> or (3) differing conformational restrictions of physisorbed **d-C17** and **d-C17SS**, whereby the attachment of the sulfur atoms to the surface of gold is more constrained for **d-C17SS** than for **d-C17**. Given that we observed similar rates of adsorption for **m-C17** and **m-C17SS** (see Figure 6), the difference in the rates of adsorption of **d-C17** and **d-C17SS** probably fails to arise from either "chemically" different rates of oxidative addition of thiol vs disulfide or contamination by oligomeric/polymeric disulfide species.<sup>55</sup> Indeed, previous kinetics studies of the adsorption of the cyclic aromatic disulfide, 2,3-dithia-6,7-dihexadecyltetralin, which remained uncontaminated with oligomeric or polymeric disulfide species, also showed slow/poor rates of adsorption relative to that of its structurally analogous dithiol.<sup>25</sup> Consequently, we propose that the rate of adsorption of **d-C17SS** is slower than that of **d-C17** because of conformational constraints imposed by the spiro geometry of the cyclic disulfide. In this proposal, we argue that the disulfide bond in physisorbed **d-C17SS** lies roughly perpendicular to the surface, which limits facile oxidative addition (or bonding) to the surface (see Figure 10a). In contrast, the disulfide bond in physisorbed **m-C17SS** probably lies roughly parallel to the surface (Figure 10b), which permits facile oxidative addition (or bonding) to the surface. Similarly, the disulfide bond in physisorbed **n-C17SS** probably lies roughly parallel to the surface (Figure 10c). In any event, the absence of the spiro geometry in **m-C17SS** and **n-C17SS** undoubtedly affords greater flexibility to the disulfide moieties of these adsorbates relative to that of **d-C17SS**, which could also rationalize the relatively slow chemisorption of **d-C17SS** onto the surface of gold.

Finally, we propose that the physisorbed geometry for **d-C17** is analogous to that for **d-C17SS** (i.e., with at least one of the thiol moieties of **d-C17** directed away from the surface, as shown in Figure 10d) and thus might be partly responsible for the observed slower rate of chemisorption for **d-C17** relative to those for **n-C17** and **m-C17** in both the fast and slow regimes. As noted above, diffusion to the surface in the slow regime



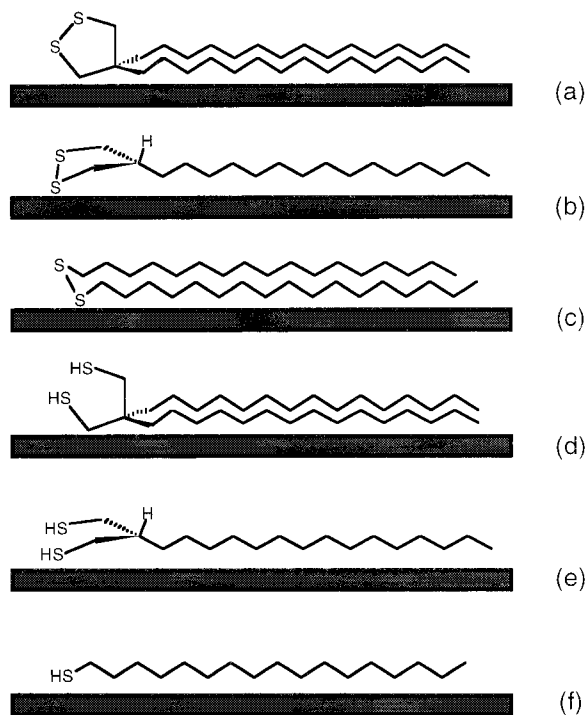


**Figure 10.** Illustration of the proposed physisorbed states of (a) **d-C17SS**, (b) **m-C17SS**, (c) **n-C17SS**, (d) **d-C17**, (e) **m-C17**, and (f) **n-C17**.

might also play a predominant role in influencing the relative rates of orientational ordering of these thiol-derived SAMs.

## Conclusions

The adsorption profiles for the formation of densely packed SAMs on gold exhibited two kinetic regimes: a fast initial adsorption wherein  $\sim 80$ – $90\%$  of each of the types of species was adsorbed, followed by a slower orientational ordering in which the alkyl chains became more crystalline. The adsorption profiles for the formation of loosely packed SAMs exhibited, in contrast, a single rapid adsorption with no detectable subsequent change. The data from the kinetics studies suggest the following trend in the rates of adsorption of the thiols: **m-C17**  $\sim$  **n-C17**  $>$  **d-C17**. The adsorption of the corresponding disulfides was either marginally or markedly slower than that of the parent thiols, depending on the structures of the adsorbates. The data from the coadsorption studies were consistent with the following trend in the thermodynamic stabilities of the thiol-derived SAMs: **m-C17**  $>$  **d-C17**  $\gg$  **n-C17**. The data from the kinetics and coadsorption studies were rationalized using a steady-state kinetic model, wherein initial physisorption was followed by chemisorption and ultimately complete monolayer formation. Relative rates of adsorption in the fast regime were consistent with the steady-state model (i.e., the rates appeared to depend both on the population of the physisorbed state and the barrier to chemisorption). Relative rates of adsorption in the slow ordering regime were perhaps additionally influenced by the rates of diffusion of the adsorbates through the partially formed monolayer films.

**Acknowledgment.** The National Science Foundation (CAREER Award to T.R.L.; CHE-9625003) and the Robert A. Welch Foundation (Grant E-1320) provided generous support for this research. We thank Professors Jonathan Friedman (University of Houston) and Watson Lees (Syracuse University) for helpful discussions.

## References and Notes

- Ulman, A. *An Introduction to Ultrathin Organic Films*; Academic Press: Boston, MA, 1991.
- Whitesides, G. M. *Sci. Am.* **1995**, *9*, 146.
- Ulman, A. *Chem. Rev.* **1996**, *96*, 1533.
- Bensebaa, F.; Boicu, R.; Huron, L.; Ellis, T. H.; Kruus, E. *Langmuir* **1997**, *13*, 5335 and references therein.
- Bucher, J. P.; Santesson, L.; Kern, K. *Langmuir* **1994**, *10*, 979.
- Sondag-Juethorst, J. A. M.; Schönenberger, C.; Fokkink, L. G. J. *J. Phys. Chem.* **1994**, *98*, 6826.
- Bain, C. D.; Troughton, E. B.; Tao, Y.-T.; Evall, J.; Whitesides, G. M.; Nuzzo, R. G. *J. Am. Chem. Soc.* **1989**, *111*, 321.
- Hähner, G.; Wöll, Ch.; Buck, M.; Grunze, M. *Langmuir* **1993**, *9*, 1955.
- Biebuyck, H. A.; Bain, C. D.; Whitesides, G. M. *Langmuir* **1994**, *10*, 1825.
- Schessler, H. M.; Karpovich, D. S.; Blanchard, G. J. *J. Am. Chem. Soc.* **1996**, *118*, 9645.
- Terrill, R. H.; Tanzer, T. A.; Bohn, P. W. *Langmuir* **1998**, *14*, 845.
- Mohri, N.; Inoue, M.; Arai, Y.; Yoshikawa, K. *Langmuir* **1995**, *11*, 1612.
- Hu, K.; Bard, A. J. *Langmuir* **1998**, *14*, 4790.
- Dannenberger, O.; Wolff, J. J.; Buck, M. *Langmuir* **1998**, *14*, 4679.
- Jung, Ch.; Dannenberger, O.; Xu, Y.; Buck, M.; Grunze, M. *Langmuir* **1998**, *14*, 1103.
- Castner, D. G.; Hinds, K.; Grainger, D. W. *Langmuir* **1996**, *12*, 5083.
- Wooster, T. T.; Gamm, P. R.; Geiger, W. E.; Oliver, A. M.; Black, A. J.; Craig, D. C.; Paddon-Row, M. N. *Langmuir* **1996**, *12*, 6616.
- Tang, X. Y.; Schneider, T. W.; Walker, J. W.; Buttry, D. A. *Langmuir* **1996**, *12*, 5921.
- Chechik, V.; Schonherr, H.; Vancso, G. J.; Stirling, C. J. M. *Langmuir* **1998**, *14*, 3003.
- Fenter, P.; Eberhardt, A.; Eisenberger, P. *Science* **1994**, *266*, 1216.
- Schlenoff, J. B.; Li, M.; Ly, H. *J. Am. Chem. Soc.* **1995**, *117*, 12528.
- Bain, C. D.; Biebuyck, H. A.; Whitesides, G. M. *Langmuir* **1989**, *5*, 723.
- Meyer, B. *Chem. Rev.* **1976**, *76*, 367. Dixon, D. A.; Zeroka, D.; Wendoloski, J. J.; Wasserman, Z. R. *J. Phys. Chem.* **1985**, *89*, 5334.
- Garg, N.; Lee, T. R. *Langmuir* **1998**, *14*, 3815.
- Garg, N.; Friedman, J. M.; Lee, T. R. *Langmuir* **2000**, *16*, 4266.
- Garg, N.; Carrasquillo-Molina, E.; Lee, T. R. *Langmuir*, manuscript submitted.
- Colorado, R., Jr.; Villazana, R. J.; Lee, T. R. *Langmuir* **1998**, *14*, 6337.
- Shon, Y.-S.; Lee, T. R. *Langmuir* **1999**, *15*, 1136.
- Shon, Y.-S.; Garg, N.; Colorado, R., Jr.; Villazana, R. J.; Lee, T. R. *Mater. Res. Soc. Symp. Proc.* **1999**, *576*, 183.
- Shon, Y.-S.; Colorado, R., Jr.; Williams, C. T.; Bain, C. D.; Lee, T. R. *Langmuir* **2000**, *16*, 541.
- Lee, S.; Shon, Y.-S.; Colorado, R., Jr.; Guenard, R. L.; Lee, T. R.; Perry, S. S. *Langmuir* **2000**, *16*, 2220.
- Shon, Y.-S.; Lee, S.; Perry, S. S.; Lee, T. R. *J. Am. Chem. Soc.* **2000**, *122*, 1278.
- The optimized C–S–S–C dihedral angles for the cyclic disulfides and the maximum distance spanned by the sulfur atoms of the chelating dithiol were determined by molecular modeling using PC Model V 5.0: Serena Software, Bloomington, IN.
- Contact angles of hexadecane are remarkably sensitive to the composition, structure, and molecular orientation of hydrocarbon interfaces: Bain, C. D.; Whitesides, G. M. *Angew. Chem., Int. Ed. Engl.* **1989**, *28*, 506.
- Nuzzo, R. G.; Dubois, L. H.; Allara, D. L. *J. Am. Chem. Soc.* **1990**, *112*, 558.
- Schreiber, F.; Eberhardt, A.; Leung, T. Y. B.; Schwartz, P.; Wetterer, S. M.; Lavrich, D. J.; Berman, L.; Fenter, P.; Eisenberger, P.; Scoles, G. *Phys. Rev. B* **1998**, *57*, 12476.
- Poirier, G. E.; Pylant, E. D. *Science* **1996**, *272*, 1145.
- Bain, C. D.; Evall, J.; Whitesides, G. M. *J. Am. Chem. Soc.* **1989**, *111*, 7155. Bain, C. D.; Whitesides, G. M. *J. Am. Chem. Soc.* **1989**, *111*, 7164.
- Purcell, K. F.; Kotz, J. C. *Inorganic Chemistry*; W. B. Saunders: Philadelphia, PA, 1977.
- Karpovich, D. S.; Blanchard, G. J. *Langmuir* **1994**, *10*, 3315.
- Peterlinz, K. A.; Georgiadis, R. *Langmuir* **1996**, *12*, 4731.
- Schneider, T. W.; Buttry, D. A. *J. Am. Chem. Soc.* **1993**, *115*, 12391.
- Shon, Y.-S.; Lee, T. R. University of Houston, Houston, TX. Unpublished observations.
- The  $\nu_a^{\text{CH}_2}$  values were checked on several different slides for immersion times  $\geq 1$  h. All measurements consistently showed higher

crystallinities for the SAMs absorbed from ethanol, thereby excluding influence from instrumental error.

(45) For example, it is possible that, relative to isooctane, ethanol destabilizes the physisorbed state (vide infra). In this scenario, alkanethiols might chemisorb directly (and thus rapidly) from ethanol without requiring the intermediacy of a physisorption preequilibrium.

(46) Lavrich, D. J.; Wetterer, S. M.; Bernasek, S. L.; Scoles, G. *J. Phys. Chem. B* **1998**, *102*, 3456.

(47) Xu, S.; Cruchon-Dupeyrat, S. J. N.; Garno, J. C.; Liu, G.-Y.; Jennings, G. K.; Yong, T.-H.; Laibinis, P. E. *J. Chem. Phys.* **1998**, *108*, 5002.

(48) Yamada, R.; Uosaki, K. *Langmuir* **1997**, *13*, 5218.

(49) Yamada, R.; Uosaki, K. *Langmuir* **1998**, *14*, 855.

(50) Laidler, K. J. *Chemical Kinetics*, 2nd ed.; McGraw-Hill: New York, 1965; pp 267–274.

(51) Although data from the coadsorption of **d-C17** and **n-C17** might offer further insight to these discussions, the indistinguishable thicknesses, wettabilities, and IR spectra of the SAMs derived from these two adsorbates presently precludes this type of study.

(52) Shon, Y.-S.; Lee, T. R. *J. Phys. Chem. B* **2000**, *104*, 8192.

(53) In coadsorption studies involving **m-C17** and **d-C17**, it is possible that **m-C17** adsorbs preferentially as a kinetically trapped species. The exchange experiments involving preformed SAMs and free thiols in solution (see ref 52), however, argue against this hypothesis.

(54) Fenter, P.; Schreiber, F.; Berman, L.; Scoles, G.; Eisenberger, P.; Bedzyk, M. J. *Surf. Sci.* **1998**, *412/413*, 213.

(55) Analysis of freshly prepared samples of **d-C17SS** and **m-C17SS** by <sup>1</sup>H NMR spectroscopy (300 MHz, CDCl<sub>3</sub>) showed no evidence of oligomeric or polymeric species. Analysis of neat samples of **d-C17SS** that were stored for several months at room temperature, however, showed CH<sub>2</sub>SS resonances attributable to ≤10% oligomeric/polymeric species at a chemical shift of  $\delta$  2.87, which was shifted to a slightly lower value relative to the parent dithiolane ( $\delta$  2.88). Given the known equilibrium constant for the formation of 1,2-dithiolanes,<sup>56</sup> trace amounts of oligomeric/polymeric species in neat samples of **d-C17SS** and **m-C17SS** are perhaps unavoidable.<sup>57</sup>

(56) Lees, W. J.; Whitesides, S. M. *J. Org. Chem.* **1993**, *58*, 642.

(57) Lees, W. J. Syracuse University, Syracuse, NY. Personal communication.